Instrument Science Report STIS 2015-05

Astrometric Performance of STIS CCD CTI Corrections on Omega Cen Images

John Biretta, Sean Lockwood, and John Debes

September 28, 2015

ABSTRACT

We are in the process of enabling pixel-based charge transfer inefficiency (CTI) corrections for the STIS CCD detector. Herein we examine the astrometric performance of these new pixel-based CTI corrections, and compare their performance to the already existing empirical CTI corrections. Tests are performed using imaging observations of the star cluster Omega Cen taken in 2012. The astrometric effects of CTI are evaluated by comparing the Y coordinates of the stars on images read out through the A and D amplifiers, which are located at opposite corners of the CCD detector. The position changes due to CTI in uncorrected data, and when normalized to 1024 parallel transfers, are ~0.02 pixel for stars near magnitude 16 to 17, and increase roughly linearly with magnitude, reaching ~0.2 pixel by magnitude 22. The empirical and pixel-based CTI corrections both work very well and give nearly identical results. Both correction methods remove 75% to 90% of the Y position change caused by CTI across all magnitudes we tested.

Operated by the Association of Universities for Research in Astronomy, Inc., for the National Aeronautics and Space Administration

1. Introduction

Charge Transfer Inefficiency (CTI) in CCD detectors causes charge to be temporarily trapped in the CCD during readout of the device, which leads to loss of counts from target images. It also causes trailing of both target images and other features such as hot pixels and cosmic ray tracks. CTI obviously affects stellar photometry as counts are removed from the core of the point spread function (PSF), but it also affects astrometry as counts are relocated from their proper position in the images, to down-stream locations (i.e. locations farther from the amplifier).

Empirical CTI corrections have been available for the STIS CCD images for many years (Goudfrooij 2006). These corrections compare the observed magnitudes and positions of stars with their true magnitudes and positions, and provide corrections which are a function of location on the detector, observed stellar counts, image background counts, and observation epoch. These are simply correction equations which can be applied to the observed magnitudes and positions.

Efforts are now underway to implement *pixel-based* CTI corrections for the STIS CCD detector (Anderson and Bedin, 2010; Lockwood, et al. 2013, 2014a, 2015). These pixel-based corrections attempt to model the detector-level physics of CTI effects, and then correct each pixel of the image to the proper counts with CTI effects removed. Pixel-based corrections have several potential advantages: besides correcting the photometry and astrometry, they can remove trails on cosmic ray hits and hot pixels, thereby reducing artifacts and the background noise in images. Pixel-based corrections can also correct target structure for complex scenes which are beyond the scope of simple empirical corrections derived from stellar images.

A previous report explored the *photometric* performance of CTI corrections for the STIS CCD detector for stellar images using observations of the Omega Cen cluster (Biretta, Lockwood, and Debes 2015, hereinafter BLD2015). Herein we test the *astrometric* performance of the corrections on some of the same data. We will employ a strategy of using images which are read-out through amplifiers on opposite sides of the CCD (Figure 1 illustrates the layout of the amplifiers). In this case we will use amplifiers A and D. As the image is read-out, CTI will cause some of the charge to trail behind the image, hence leading to a shift in the Y position of the star in the direction away from the amplifier. Since amplifiers A and D are read out in opposite directions and cause trailing in opposite directions, differencing the position of the star as read out through amplifier A and amplifier D, will yield the astrometric position shift attributable to CTI effects.

The primary goal of this report is to test the effectiveness and accuracy of the new pixel-

based CTI corrections, both relative to the established empirical corrections, and in absolute terms of removing CTI effects. The results herein will also aid observers in assessing the astrometric accuracy of their own data, both before and after CTI corrections are applied.

Section 2 of this report describes the data sets used, Section 3 describes the image processing performed, and Section 4 discussed the astrometric measurements. The results are presented and discussed in Sections 5 and 6, respectively. The final section discussed possible future enhancement to this work.

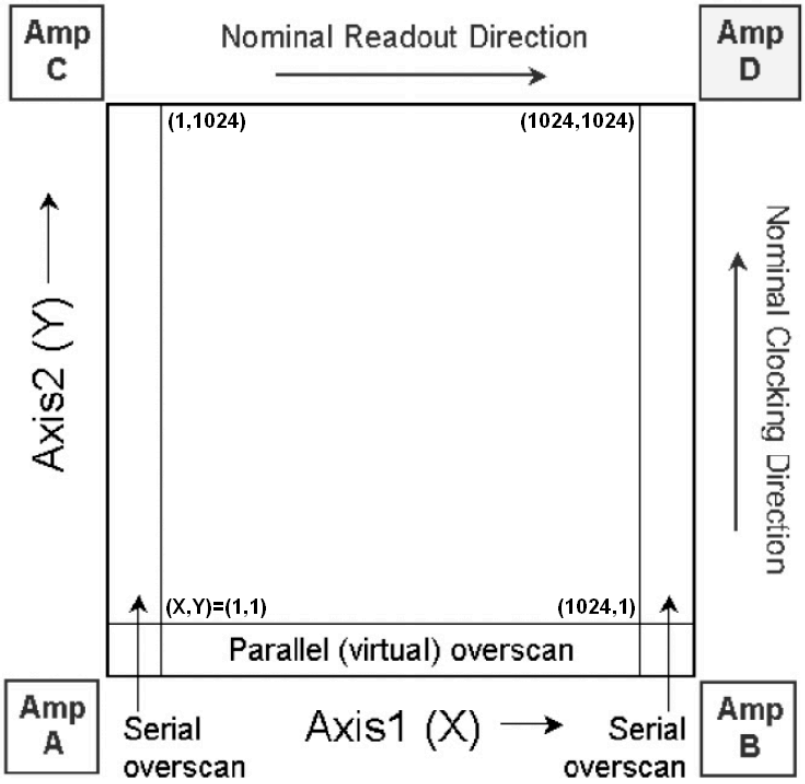

Figure 1. Locations of the A and D amplifiers. Coordinates (X,Y) of the image corners are as indicated. Amplifier D (top right) has the lowest read noise, and is the default amplifier for all science observations. From Goudfrooij, et al., 2006.

2. The Data

Table 1 lists the two Omega Cen images used herein. These images were selected since their dates are near the middle of the STIS post-recovery era (2009-2015), and should be typical of recent STIS CCD observations. Both images utilize the CLEAR filter, the 50CCD aperture, the MIRVIS grating, and are taken at CCDGAIN=4. Each exposure consists of two sub-frames with the individual exposure time listed as MEANEXP, and total exposure time listed as TEXPTIME. The entry PA_APER gives the position angle of the aperture on the sky.

Table 1. Omega Cen images used herein.

Image Name	Prop ID	DATE-OBS	MEANEXP (sec)	TEXPTIME (sec)	PA_APER (deg)	CCDAMP
obuo01050_sx2.fits	12770	2/10/2012	30	60	-94.98	D
obuo01090_sx2.fits	12770	2/10/2012	30	60	-94.98	A

3. Image Processing

The "D" amplifier image utilzed the normal pipeline calibration and reference files. However amplifier "A" is generally not used by observers, and hence no reference files were available. It was necessary to create special reference files for the amp A image. A bias reference file was created from 18 amp A gain 4 bias frames taken between 12/1/2011 and 3/10/2012, which bracketed the Omega Cen data. Usually dark calibration is performed using dark files taken during the same week as the target observation, but no such dark frames were available. Instead, an amp A dark reference file was created from eight amp A gain 1 dark frames taken between 12/2/2011 and 12/19/2011 – these were the closest in time available.[1] This dark reference file was scaled to gain 4 of the Omega Cen data, and then subtracted.[2] The geometrically rectified *_sx2.fits products were used for all tests. The calibrated amp A and amp D images used to test the un-corrected and empirically corrected cases are shown in Figure 2.

For the pixel-based corrected case, the data were manually processed as follows. First the

[1] These dark calibration frames were bias-calibrated using an amp A gain 1 bias reference file constructed from 15 bias frames taken between 11/1/2011 and 1/11/2012.

[2] The primary impact of the large time interval between amp A calibration files and Omega Cen data, is that warm and hot pixels will be poorly corrected during dark calibration. This contributes random negative and positive pixels to the amp A image which will act as a noise source. It will primarily impact faint stars where large numbers of poorly subtracted warm pixels contribute noise-like errors. We do not expect it to introduce any systematic errors in our astrometric measurements.

normal BIASLEV, BIASCORR, and DQICORR calibrations were applied using the BASIC2D task in the STIS STSDAS package. Pixel-based CTI corrections were then applied using the StisPixCteCorr python task, along with the reference file TEST_PCTE.FITS. Details of the STIS pixel-based CTI corrections are presented elsewhere (Lockwood, et al., 2012, 2013, 2014a, 2014b, 2015). Our user settable parameters in the CTE reference file header are listed in Table 2 (see BLD2015 for a full discussion of the parameters). Finally the remaining standard calibrations (DARKCORR, FLATCORR, etc.) were applied using CALSTIS. In all cases the normal pipeline / archive reference files were used.[3]

Table 2. TEST_PCTE.FITS parameters.

Parameter	Value
SIM_NIT	7
SHFT_NIT	4
RN_CLIP	5.6
NSEMODEL	0
SUBTHRSH	-200

[3] We did not apply pixel-based CTI corrections to the dark reference files. We ran a test using CTI-corrected darks for one image, and found it did not significant alter the photometry or astrometry. For long exposures this would reduce artifacts and improve the signal-to-noise ratio, but for our short exposures there was no significant impact on the results.

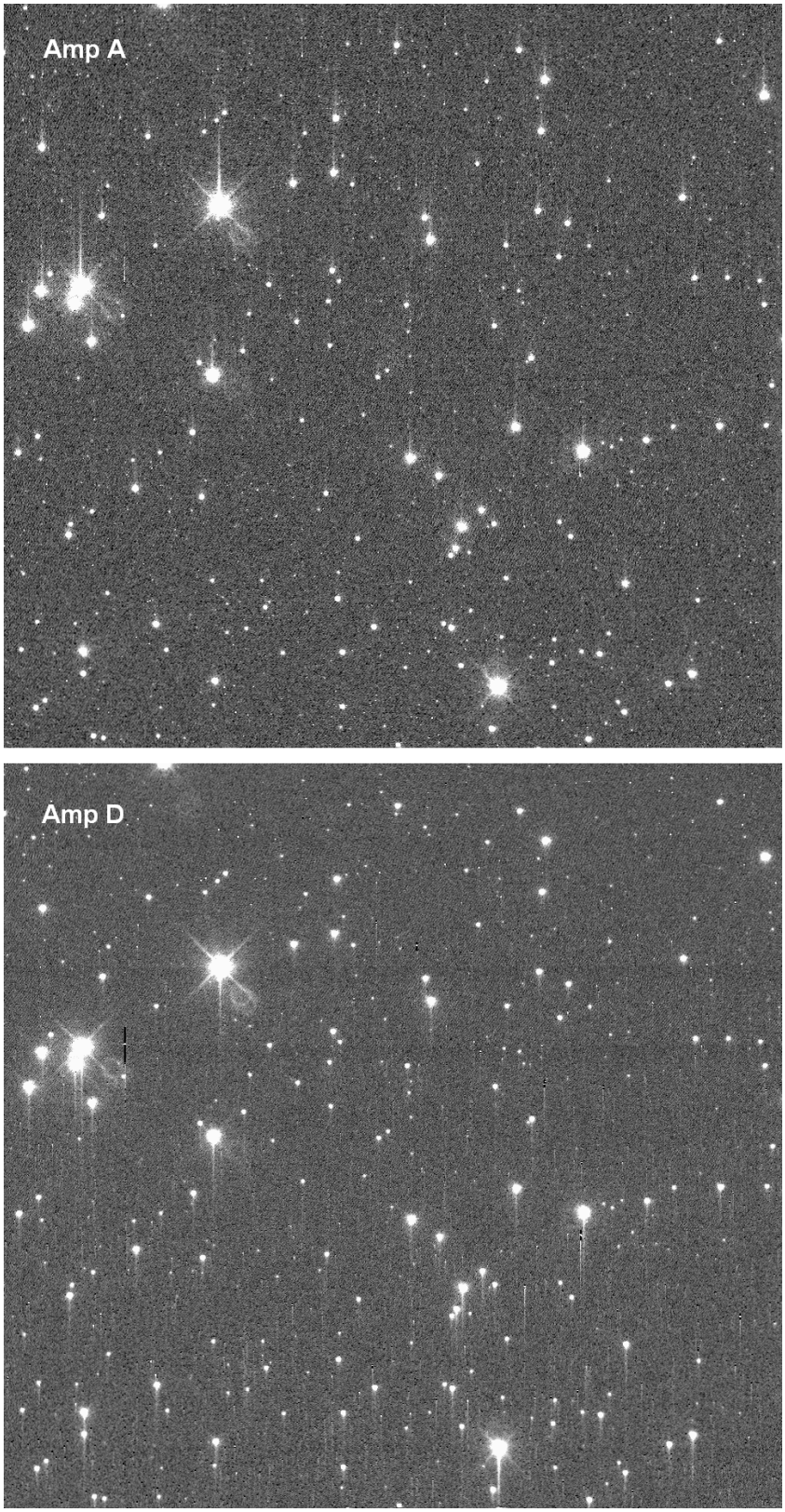

Figure 2. Calibrated but uncorrected amp A (obuo01090_sx2.fits) and amp D (obuo01050_sx2.fits) images.

The pixel-based CTI corrections for the amp A data require some additional explanation. These were pixel-based corrected by assuming they had the same corrections as the amp D data. This is a reasonable assumption, since the CTI effects occur on surface of the CCD detector, and should be independent of the amplifier properties. Other properties, like the read-out speed, are identical between amps A and D. The amp A data were bias calibrated, the rows were flipped in the Y-direction (row [X,1] was moved to row [X,1024], etc.), the pixels were loaded into an amp D image fits file, and then the pixel-based CTI corrections were calculated in the usual way. After CTI correction the image rows were flipped back to the normal arragement, and the remaining calibrations (flat fielding, cosmic ray rejection, etc.) were applied.

The calibrated images with pixel-based CTI corrections applied are shown in Figure 3. Most of the CTI trails on stars have been removed, though some residual trailing remains on the three or four brightest stars. The amp A image has higher background noise due to poorer bias and dark calibration, since contemporaneous calibration data were not available. The background noise also tends to be higher far from the amplifier in both the amp A and amp D images, due to amplification of the noise by the pixel-based CTI correction algorithm. The correction algorithm is making larger corrections in these regions far from the amplfier, and for the same reason, it has greater noise amplification far from the amplifier.

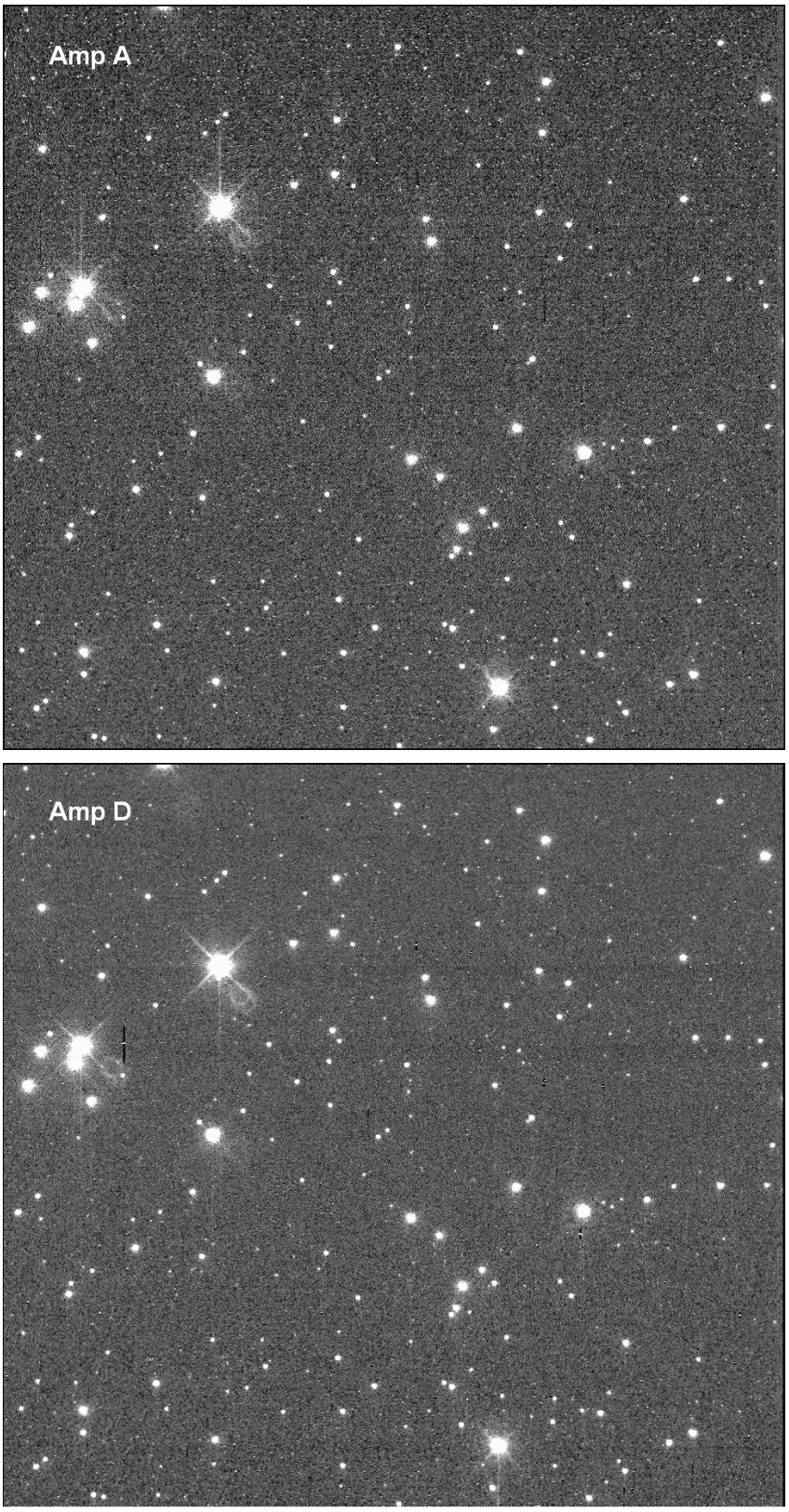

Figure 3. Calibrated and pixel-based CTI corrected images for amp A (obuo01090_sx2.fits) and amp D (obuo01050_sx2.fits).

4. Astrometry

We used the stellar photometry procedures described by Roman-Duval and Proffitt (2013, hereinafter RP2013) and BLD2015. These procedures output both a magnitude for the star, and a fitted (X,Y) position. The star catalog from BLD2015 is used.

Magnitudes were determined by aperture photometry using the IDL APER procedure with an aperture radius of 5 times the FWHM of the PSF. The sky annulus had the same inner radius, and a thickness of 5 pixels. The nominal PSF FWHM was about 1.8 pixels, leading to an aperture radius of about 4.5 pixels. The star positions were derived using the IDL CENTROID routine.

Star images were checked for saturation effects. The brightest star contained ~36,000 DN in the central pixel of the PSF, and so slightly exceeds the 130,000 e- full-well. While accurate photometry can still be performed (e.g. Gilliland, Goudfrooij & Kimble, 1999), we were concerned that astrometric shifts might be induced, and hence omitted this star.

The data were further edited by discarding stars within a 100 pixel border around the edges of the image. This border excludes regions where the star aperture or sky annulus might be impacted by the 50CCD aperture mask. It also serves to exclude the 38 pixel empty border of the 1100x1100 pixel *_sx2.fits files.

We also compared the X positions of the stars in the amp A and amp D images. In a few cases the X positions of the stars were different by several pixels, which we attribute to the data being corrupted by nearby hot pixels. These stars were also discarded.

The empirical CTI corrections were calculated using the equations in Goudfrooij, et al., 2006. These corrections depend on the average star counts (in e-) in the individual sub-frames or IMSETs of the observation, the average counts per pixel in the sky annulus (in e-/pixel)[4], the Y position of the star on the detector, and the observation date. These corrections were applied to the (X, Y) positions from the IDL CENTROID routine, which was run on the un-corrected images.[5] For the pixel-based corrected case we simply run the

[4] The sky background in the individual 30 second frames was approximately 3 electrons per pixel.
[5] We did not use the STSDAS CTESTIS program for this calculation as an error was found in that program (version Jan2013). Apparently CTESTIS computes the correction to the star Y-position as if it were at the center of the detector (Y=512) regardless of the actual position of the star. Herein we use the Goudfrooij, et al., 2006 equations and linearly scale the correction given at Y=512 to match the measured Y-position of the star.

same photometry and astrometry scripts on the images with pixel-based CTI corrections applied.

The astrometric information collected above was then used to evaluate the CTI corrections. The quantity we test is the Y position difference of each star between the amp A and amp D images, which can be written as [Y(amp A) – Y(amp D)].[6] In the absence of any CTI effects, we should obtain the same positions for the star regardless of the amplifier, and hence we expect to see [Y(amp A) – Y(amp D)] = 0 for all stars. When CTI is present, star images in the A amplifier image will trail upwards on the detector and hence have a positive shift (e.g. Figure 1). Similarly star images will trail downwards in the D amplifier, towards smaller Y values. Hence when CTI is present we expect the difference [Y(amp A) – Y(amp D)] to be positive.

Furthermore, if we assume the size of the CTI effect is the same for amplifier A and amplifier D, and further that the effect is linear with distance to the amplifier, we can show that [Y(amp A) – Y(amp D)] will equal the astrometric shift for a star read out across the full detector (1024 rows). If we let $\Delta Y_{CTI,\,1024}$ represent position shift for a star read out across the full 1024 rows of the detector, and let Y represent the true centroid of the star on the detector, the measured positions for the two amplifiers are:

$$Y(\text{amp A}) = Y + \Delta Y_{CTI,\,1024} * Y/1024$$

$$Y(\text{amp D}) = Y - \Delta Y_{CTI,\,1024} * (1024\text{-}Y)/1024$$

And hence

$$[Y(\text{amp A}) - Y(\text{amp D})] = \Delta Y_{CTI,\,1024}$$

This quantity is independent of the star's position on the detector. We expect that $\Delta Y_{CTI,\,1024}$ will have the usual dependencies for CTI, namely that the position shift will increase as total counts in the star decreases, as background counts per pixel in the image decrease, and increase for later epochs. For a situation such as we have here, with two images at the same epoch and same background, $\Delta Y_{CTI,\,1024}$ depends only on the brightness of the star.

The error bars on [Y(amp A) – Y(amp D)] are estimated from the photon noise and flat field errors. The sizes of the error bars have also been checked against the differences in

[6] Goudfrooij, et al., 2006 use a similar calculation with amp B and amp D to derive the empirical CTI corrections for astrometry.

the measured X positions of the stars, which should have similar uncertainties to the Y coordinates, but are much less affected by CTI.

A possible error source in our measurements is any pointing change of the telescope, or motion of the internal STIS optics, between the amp A and amp D images. Any such errors would create a constant offset in the values of [Y(amp A) – Y(amp D)]. Our images were obtained on the same HST orbit and same target acquisition, and used two-FGS mode, which reduces the likelihood of pointing changes. We have examined the Fine Guidance Sensor (FGS) data (so-called jitter or .jit files) for our exposures. The HST pointing change along the STIS Y axis for the dominant guide star was +0.001 pixel between the amp D and amp A exposures. This suggests excellent pointing stability. However, we cannot completely rule out the possibility of image scale changes (due to OTA breathing) and other motions between the FGS and STIS. The internal motions of the STIS optics, due to thermal effects, etc., are more difficult to assess. Figure 16-3 in Proffitt, et al., 2013 illustrates the STIS CCD internal optical stability in the Y direction across two orbits. Over the middle portion of visibility periods, such as we have for our data, the stability appears to be ~0.01 pixel or better. However position excursions approaching 0.05 pixel are seen at the start of the visibility periods. Given their data cover only two orbits, and not a statistical sample, a firm conclusion is probably not possible. Herein we will assume that HST pointing and STIS optical stability errors are small (~0.01 pixel). But we must also keep in mind that some larger motion of STIS in the HST focal plane, or motion internal to STIS, is possible.

Differences in gain between the A and D amplifiers was mentioned in BLD2015. This only affects the overall conversion from detected counts to detected electrons in each amplifier. While this affects photometry, it would have no effect whatsoever on the image positions or structural details of the images. It might have some small effect on the magnitude values used in plotting the results, but the effect would only be a few percent and would be unimportant.

5. Results

Figure 4 shows the results for data without CTI corrections. Each point represents a single star in the Omega Cen images. The quantity [Y(amp A) – Y(amp D)] = $\Delta Y_{CTI,\ 1024}$ is plotted against magnitude. We recall that $\Delta Y_{CTI,\ 1024}$ is the position shift which would occur for readout of the image across 1024 detector rows. Here we have used the

magnitude without CTI corrections, and averaged the magnitude derived from the amp A and amp D data.[7]

As we see in Figure 4, the position shifts due to CTI are very small for brighter stars, being a few x 0.01 pixel in the magnitude 15 to 18 range. The CTI effects increase roughly linearly with stellar magnitude, and reach an average ~0.2 pixel near magnitude 22.

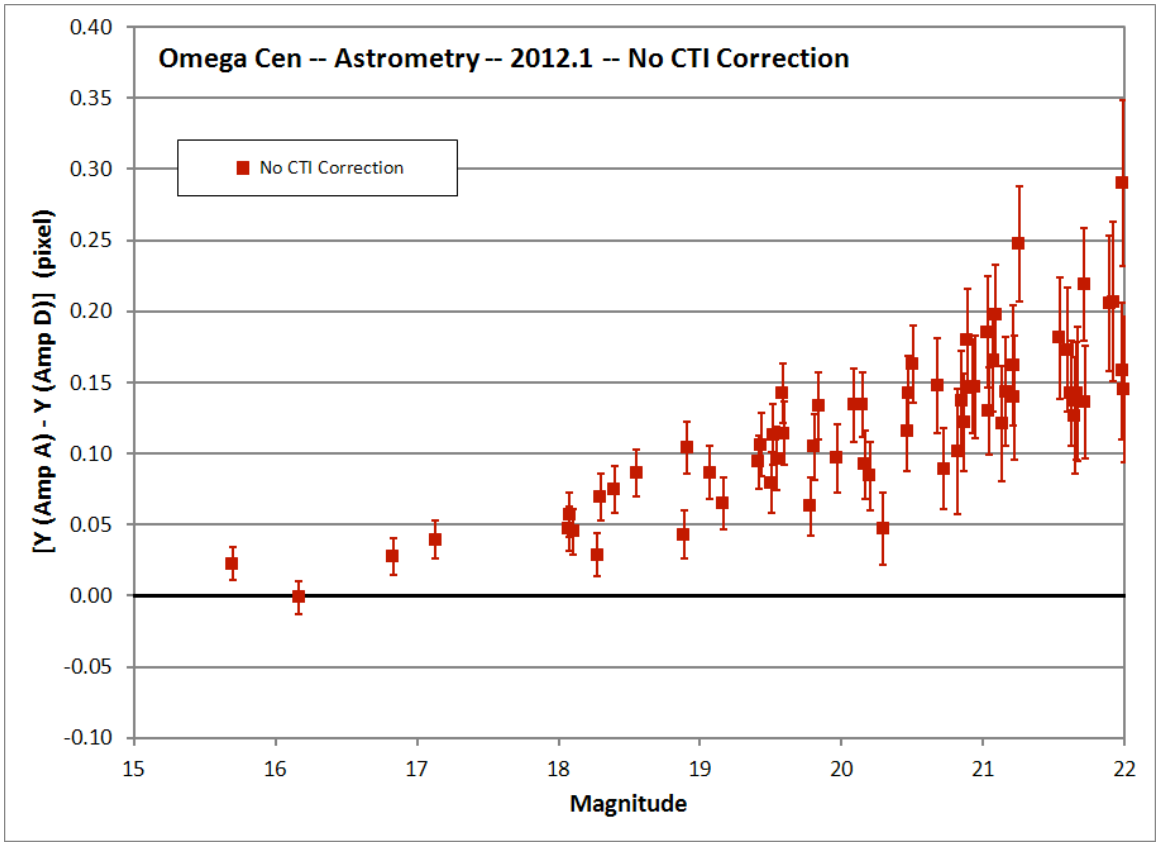

Figure 4. Plot of [Y(Amp A) – Y(Amp D)] vs. Magnitude for data without CTI corrections.

[7] The largest photometric effects due to CTI are ~0.25 magnitude for 1024 parallel transfers at magnitude 22 (BLD2015). Ignoring the CTI effects on the magnitudes does not significantly impact our astrometric results.

Figure 5 shows the results when the empirical corrections from Goudfrooij, et al., 2006 are used. The corrections appear quite successful in removing the position shifts associated with CTI, and leave only a slight average positive shift of a few x 0.01 pixel at fainter magnitudes.

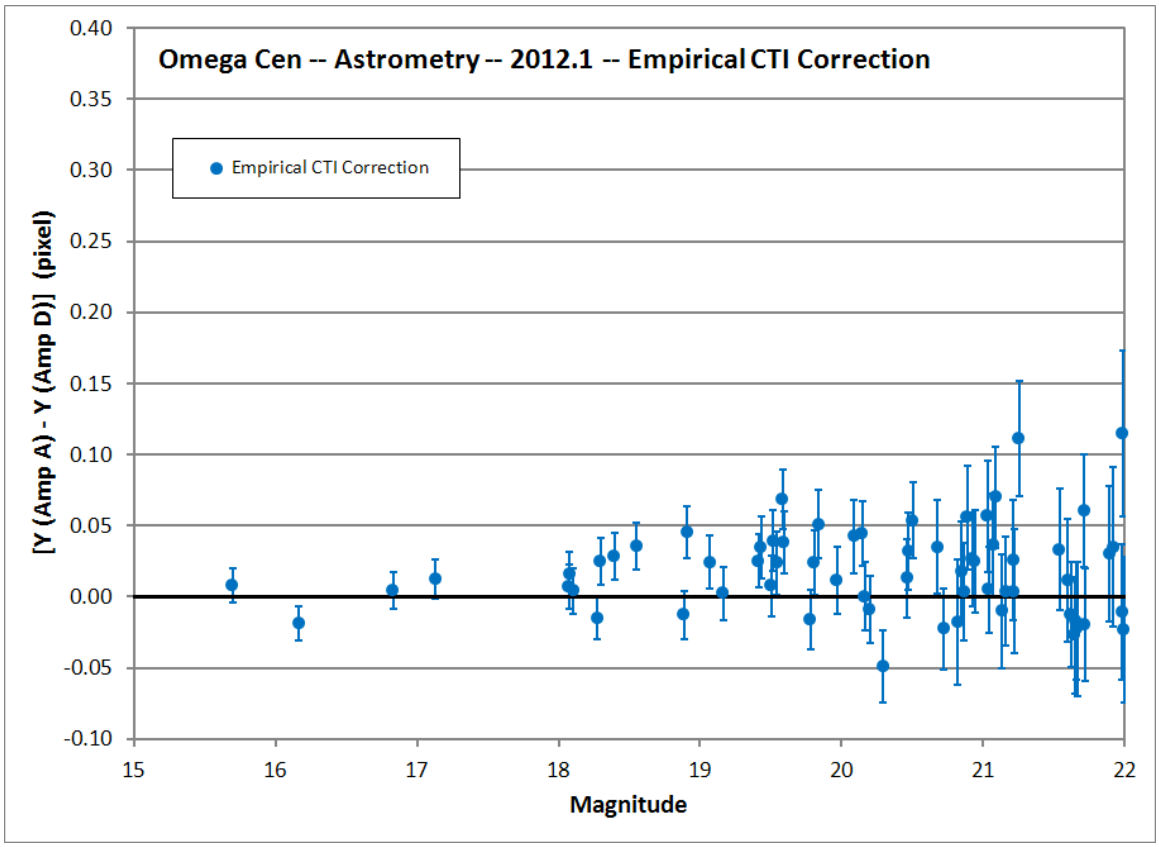

Figure 5. Plot of [Y(Amp A) – Y(Amp D)] vs. Magnitude for data with empirical CTI corrections.

Figure 6 shows the results when the pixel-based empirical CTI corrections are used. Like the empirical corrections, the pixel-based corrections are also very successful in

removing most of the position shift associated with CTI, and again leave only a slight average positive shift of a few x 0.01 pixel at fainter magnitudes.

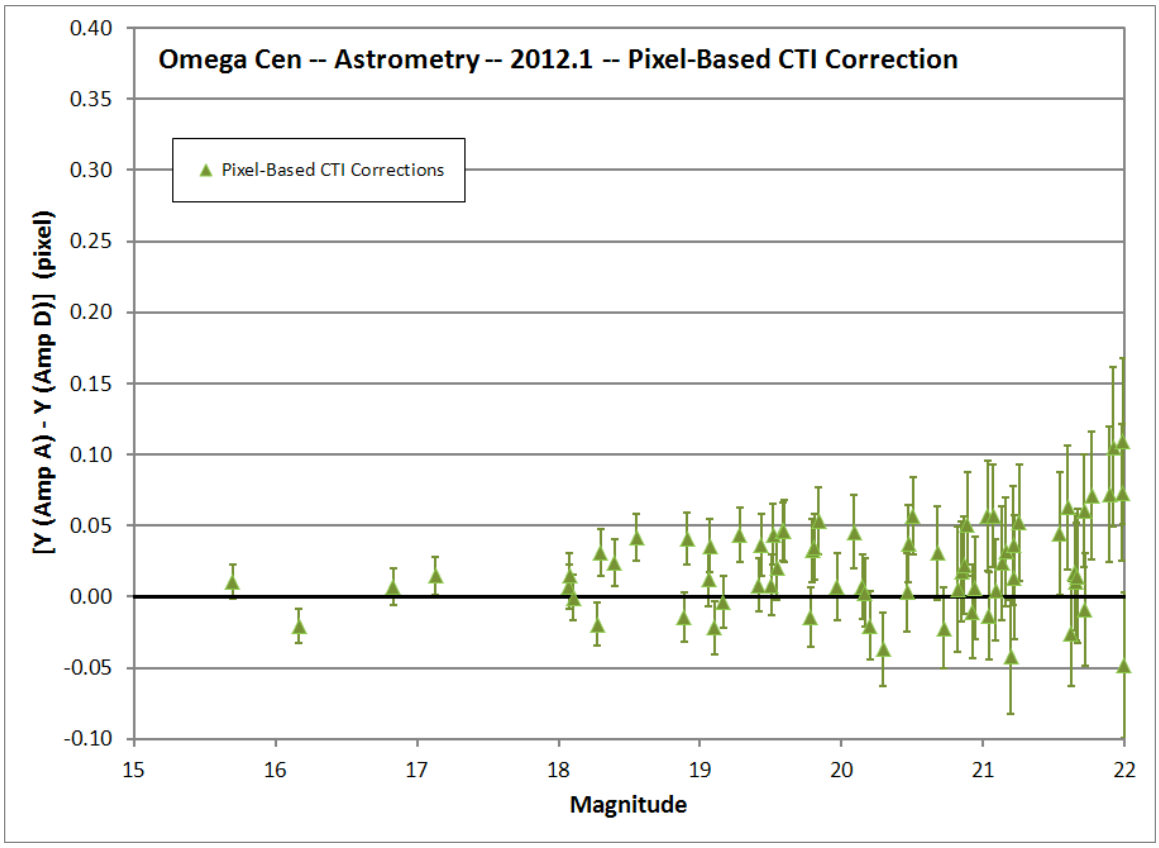

Figure 6. Plot of [Y(Amp A) – Y(Amp D)] vs. Magnitude for data with pixel-based CTI corrections.

Figure 7 shows the results for all three correction states, where the data have been binned and averaged by magnitude. The data brighter than magnitude 18 have been averaged into a single bin, since there are few data points. At fainter magnitudes we use one-

magnitude bins. Uncertainties are estimated from the scatter in the data points, and represent the uncertainty on the mean value.[8] The values are also tabulated in Table 3.

We see that the new pixel-based corrections have performance very similar to the established empirical corrections. Both correction methods remove 75% to 90% of the astrometric shift associated with CTI effects. Also, the accuracy is similar across all the magnitude bins in Figure 7.

As discussed earlier, we cannot completely rule out the possibility of HST pointing instability or STIS internal optical instability which could move the amp A and amp D images relative to each other by a few x 0.01 pixel. This would have the effect of moving the vertical scales in Figure 4 to Figure 7 by a few x 0.01 pixel. There is no direct evidence for such an offset, but it cannot be ruled out. Such an offset would increase or decrease our assessment of the CTI correction accuracy. If [Y(amp A) – Y(amp D)] decreased by a few x 0.01 pixel, it would move the corrected points closer to zero shift, and make the CTI corrections appear more accurate. While an increase by a similar amount would make them appear somewhat less accurate. Nonetheless, it would remain true that the empirical and pixel-based corrections have nearly identical performance for correcting astrometric CTI effects, and correct most of the astrometric CTI effects.

[8] The uncertainty on an individual measurement, rather than on the mean, is simply error bar on the plot (or in Table 3) times the square root of the number of data points in the bin. This later value is at the bottom of Figure 7. For example, for the 21 to 22 magnitude bin, the uncertainty on an individual point would be sqrt(22)*0.009=0.04 pixel.

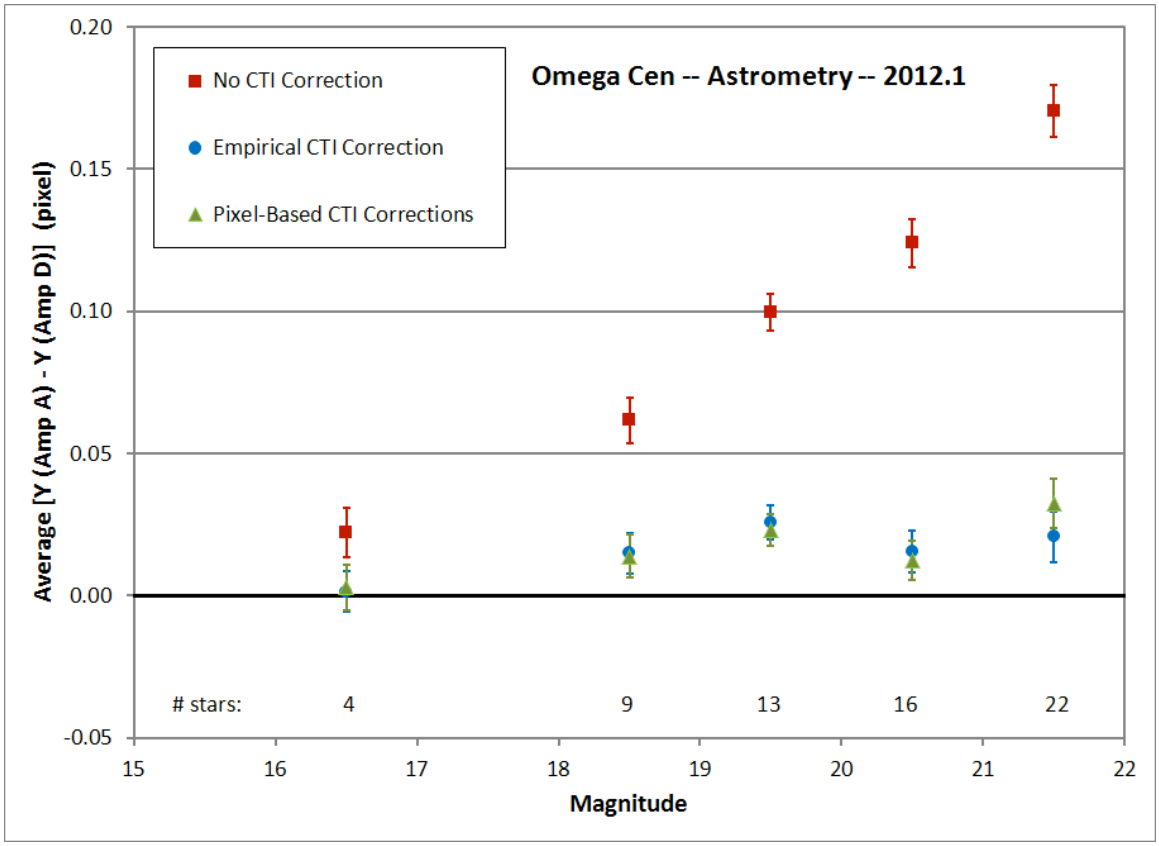

Figure 7. Plot of [Y(Amp A) – Y(Amp D)] vs. Magnitude for uncorrected, empirically corrected, and pixel-based corrected data. The data in Figures 3, 4, and 5 have been averaged into five bins by magnitude range: 15-18, 18-19, 19-20, 20-21, and 21-22. The number of stars in each bin is given near the bottom of the plot. The quantity on the vertical axis, [Y(Amp A) – Y(Amp D)], is effectively the astrometric shift expected for 1024 parallel transfers.

Table 3. Measured average position shift [Y(amp A) – Y(amp D)] = $\Delta Y_{CTI,\,1024}$ (pixels).

	CTI Correction		
Magnitude Range	None	Empirical	Pixel-Based
15-18	0.022 ± 0.009	0.001 ± 0.007	0.003 ± 0.008
18-19	0.062 ± 0.008	0.015 ± 0.007	0.014 ± 0.008
19-20	0.100 ± 0.007	0.026 ± 0.006	0.023 ± 0.006
20-21	0.124 ± 0.008	0.016 ± 0.007	0.012 ± 0.007
21-22	0.171 ± 0.009	0.021 ± 0.009	0.032 ± 0.009

As a check on our measurements, we have made similar analyses on the X-coordinates of the stars. The results are presented in Figure 8 where we plot the average X position shift [X(amp A) – X(amp D)] vs. magnitude for the stars. This plot is fully analogous to Figure 7 for the Y-coordinates. Three significant points can be made about the X position shifts in Figure 8. First, the X-coordinates appear to be independent of magnitude. This helps to confirm that the Y-coordinate variations we observe are indeed related to the parallel CTI effects. Secondly, the average position shift is not zero; instead it averages -0.105 pixel and is consistent with this value at all magnitudes. The most likely explanation of this shift is motion of the target on the detector between the amp A and amp D images, which could potentially be caused by instability in the internal STIS optics.[9] Proffitt, et al., 2013 in their Figure 16-2 show that the optical stability in the X direction is much poorer than in the Y direction. In fact, for both of their orbits there is a steady X motion of about -0.28 pixel/hour at the middle of the visibility period. If our images experienced the same drift rate, this would imply about -0.093 pixel motion between our amp A and amp D observations (amp A was observed 19 minutes after amp D), which is close to the -0.105 pixel shift we observe. Third and finally, the error bars on the points, which represent the standard deviation of the mean, are similar to those for the Y-coordinates in Figure 7, which helps to confirm the estimated uncertainties.

[9] We have also plotted [X(amp A) – X(amp D)] vs. X, and also vs. Y, and there are no strong variations in either case. This is also consistent with motion of the target on the detector between the amp A and amp D exposures.

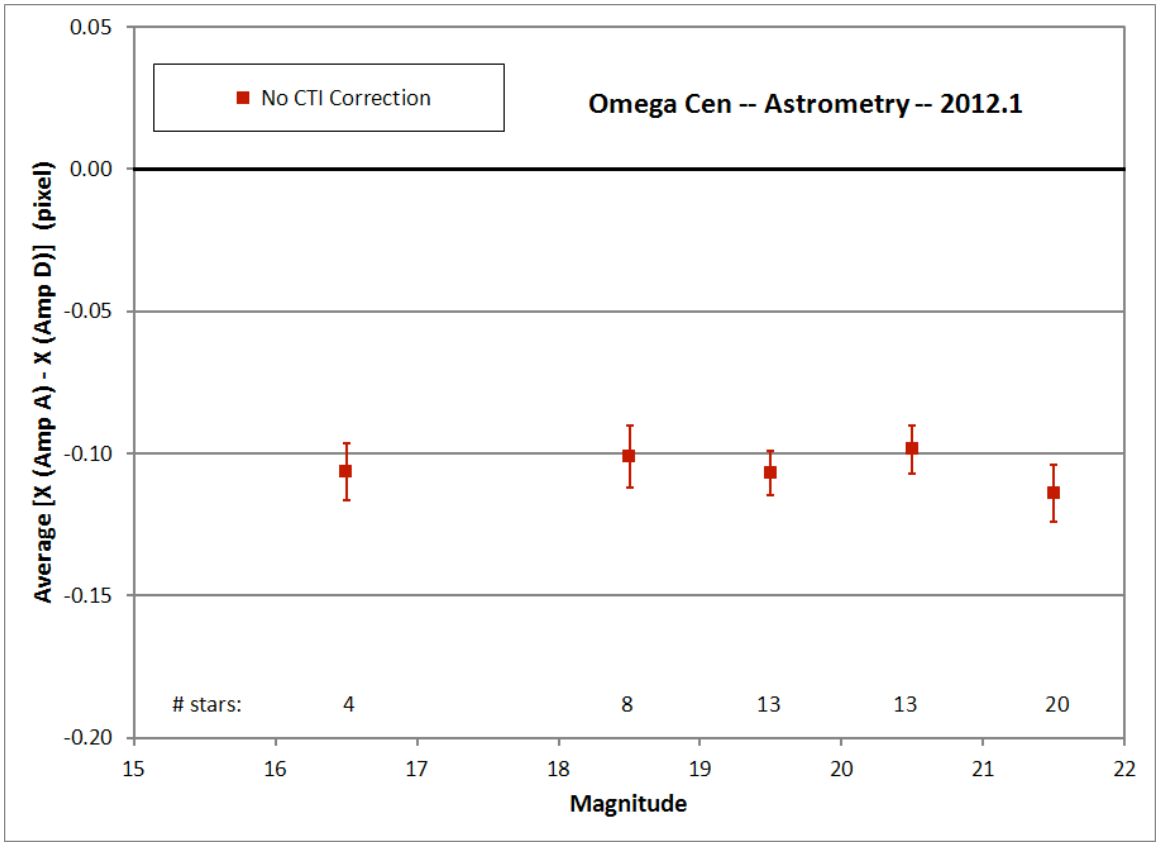

Figure 8. Plot of [X(Amp A) – X(Amp D)] vs. Magnitude for uncorrected data. The data have been averaged into five bins by magnitude range: 15-18, 18-19, 19-20, 20-21, and 21-22. The number of stars in each bin is given near the bottom of the plot.

6. Discussion

From Figure 7 and Table 3 it appears that the established empirical CTI corrections, and new pixel-based corrections, both work remarkably well in correcting the astrometric effects of CTI. Approximately 75% to 90% of the CTI effects have been removed. One of our primary goals here has been to test the new pixel-based CTI corrections relative to the long-established empirical corrections; we find that the two corrections work equally well in correcting the astrometric effects of CTI. In addition, there are no large trends in the performance vs. stellar magnitude -- the two corrections work similarly well at all magnitudes.

It is interesting that the behavior of the empirical corrections and pixel-based corrections are somewhat different for astrometry and photometry (Figure 7 herein, vs. Figure 10 and

Figure 14 in BLD2015). Here both the empirical and pixel-based corrections agree very well, and are removing 75% to 90% of the astrometric CTI effects. But for photometry, they sometimes corrected only 50% or 60% of the CTI. Moreover, the empirical corrections tended to over-correct the CTI, and the pixel-based corrections tended to under-correct CTI, whereas here they have nearly identical behaviors here for astrometry.

Astrometry and photometry however have different sensitivities to CTI effects, and this may account for these differences. The astrometric information for a star is primarily contained in a few pixels in the PSF core – in particular a few pixels immediately above and below (+Y and –Y) the center of the star where the Y-slope of the PSF is steepest. On the other hand, photometry is sensitive to counts in the entire target aperture, as well as counts the surrounding sky aperture. Photometry can be strongly affected by counts in the extended CTI tail, whereas the extended tail has little or no effect on astrometry. This might help explain the somewhat different behaviors of the corrections with regards to astrometry and photometry.

We also note that photometry and astrometry have very different sensitivities to error sources. For faint objects, accurate determination of the sky background is of critical importance, but for astrometry this is completely unimportant. Residual hot pixels which result from poor dark calibration are likely to have greater effects for photometry where both the target and sky apertures can be impacted. Residual hot pixels are an important error source especially for the amp A images, where no contemporary darks frames were available.

It is interesting to compare the accuracy of our pixel-based astrometric corrections to those derived for other HST instruments. This comparison is made somewhat difficult by the different detector formats, and the differing strength of CTI for the different instruments. Stars in our faintest magnitude bin (mag~21.5) have ~540 electrons in the central pixel of the point spread function for the individual 30s sub-exposures, a background of ~3 e-/pixel, and experience a position shift due to CTI of ~0.17 pixels (Figure 7, Table 3) for 1024 transfers. After pixel-based correction there is a residual *under*-correction of 0.03 ± 0.01 pixel, or about 19% ± 6% of the CTI effect. Anderson and Bedin (2010) discuss pixel-based corrections for the Advanced Camera for Surveys (ACS). Their closest comparable case in terms of shift across 1024 rows and image background is the central pixel ~50 e- case in their Figure 14 for 10s exposures (background ~2 e-/pixel). Their data show a shift of ~0.16 pixel across 1024 rows, which after pixel-based correction becomes an *over*-correction of ~0.02 pixel or ~13% of the CTI effect. On the other hand, another similar case for a central pixel ~20 e- shows a shift of ~0.21 pixel across 1024 rows, which after correction becomes ~0.04 pixel, or an *under*-correction or ~20% of the CTI effect. If we instead we try to match central pixel

brightness of the ACS data to our STIS data, their case closest to ours is the central pixel 316 e- case with a shift of ~0.09 pixel across 1024 rows, which after correction shows an *over*-correction of ~0.014 pixel, or ~16% of the CTI effect. Hence, while it is difficult to make direct comparisons between instruments, our residual errors after pixel-based CTI correction appear roughly comparable to those for ACS.

7. Future

There are other epochs of Omega Cen observations with pairs of amplifier A and D data already in hand that could be processed. These should probably be processed and tested when more time is available, and might give added confidence in the results. These might, for example, give more statistics on the role of any pointing changes between the amp A and amp D images.

It would be very helpful to take amp A bias and dark frames at the same time as future Omega Cen data. This would greatly improve the calibration of the amp A data, and aid removal of hot pixels, which are an important source of error for the fainter stars. While amp D is the default amplifier used for science, and is very well calibrated with two 1100s dark frames taken every day, there are only a handful of darks taken annually in amp A.

It may also be helpful to take the amp A and amp D data closer in time (i.e. less than the 19 minutes for the data presented here), so as to minimize possible pointing drifts and internal STIS optical motions between the amp A and amp D data. A simple re-ordering of the exposures in future calinbration programs is all that would be needed.

There are more faint stars availble in the images presented here (magnitude > 22), but their uncertainties would be large, and it is not clear whether there are enough numbers of faint stars so as to average-out the increased scatter.

We have assumed the pixel-based CTI corrections for amp A are identical to those for amp D. This is a reasonable assumption, given that CTI arises on the surface of the CCD detector, and should be independent of the amplifier. But it would be useful to test this assertion in the future. Separate CTI corrections could be derived using hot pixels in amp A dark frames, and compared to the amp D corrections.

Finally, it may be useful to adjust the pixel-based CTI correction parameters to see whether further improvements in their performance can be made. The photometric performance, of course, would also need to be taken into account during any adjustment.

We thank Julia Roman-Duval for providing her IDL photometry code, and for her patience while answering many questions related to the code. We also thank Charles Proffitt and Jay Anderson for many helpful discussions, and George Becker for insightful comments on a draft of this report.

References

Anderson, J., and Bedin, L. R., 2010, "An Empirical Pixel-Based Correction for Imperfect CTE. I. *HST's* Advanced Camera for Surveys," PASP, 122, 1035.

Bohlin, R. C., and Goudfrooij, P., 2003, "An Algorithm for Correcting CTE Loss in Spectrophotometry of Point Sources with the STIS CCD," Instrument Science Report STIS 2003-03R.

Chiaberge, M., Lim, P.-L., Kozhurina-Platais, V., and Sirianni, M., 2009, "Updated CTE photometric correction for WFC and HRC," Instrument Science Report ACS 2009-01.

Gilliland, R., Goudfrooij, P., and Kimble, R. A., 1999, "Linearity and High Signal-to-Noise Performance of the STIS CCD," PASP 111, 1009.

Goudfrooij, P., Bohlin, R. C., Maiz-Apellaniz, J., and Kimble, R. A., 2006, "Empirical Corrections for Charge Transfer Inefficiency and Associated Centroid Shifts for STIS CCD Observations," PASP 118, 1455.

Lockwood, S., 2012, "STIS CTE Parameter Fitting," https://confluence.stsci.edu/download/attachments/50631094/Lockwood%20--%20CTI_parameter_model_whitepaper.pdf?api=v2, internal report.

Lockwood, S., et al., 2013, "Towards a Pixel-Based CTE Correction of the STIS CCD," https://confluence.stsci.edu/download/attachments/50631094/Lockwood%20--%20AAS%20Poster%202013-01.pdf?api=v2, AAS Meeting #221.

Lockwood, S., et al., 2014a, "Progress Towards a STIS Pixel-Based CTI-Correction," HST Calibration Workshop, https://confluence.stsci.edu/download/attachments/50631094/Lockwood%20--%20Cal%20Workshop%202014-08.pdf?api=v2, http://www.stsci.edu/institute/conference/cal14/posters/Progress-Toward-a-STIS-Pixel-Based-CTI-Correction.pdf.

Lockwood, S., 2014b, "Fine-Tuning the CTI Correction Parameters," https://confluence.stsci.edu/download/attachments/50637560/cti_fine_tuning_v2.pdf?version=1&modificationDate=1422316072000&api=v2, internal report.

Lockwood, S., et al. 2015, "Pixel-Based CTI Corrections for the STIS CCD," Instrument Science Report STIS 2015-xx, in preparation.

Proffitt, C., et al., 2013, "Summary of the Results of STIS SMOV4 Calibration Activities," Instrument Science Report STIS 2013-04.

Roman-Duval, J., and Proffitt, C., 2013, "Full-field sensitivity and its time-dependence for the STIS CCD and MAMAs," Instrument Science Report STIS 2013-02 (RP2013).

Stys, D. J., Bohlin, R. C., and Goudfrooij, P., 2004, "Time-Dependent Sensitivity of the CCD and MAMA First- Order Modes," Instrument Science Report STIS 2004-04.